Journal of Power Sources 194 (2009) 1222–1225

Contents lists available at ScienceDirect

Journal of Power Sources

journal homepage: www.elsevier.com/locate/jpowsour

Short communication

A new cheap asymmetric aqueous supercapacitor: Activated carbon//$NaMnO_2$

Q.T. Qu[a], Y. Shi[a], S. Tian[a], Y.H. Chen[a], Y.P. Wu[a,*], R. Holze[b,**]

[a] Department of Chemistry & Shanghai Key Laboratory of Molecular Catalysis and Innovative Materials, Fudan University, Shanghai 200433, China
[b] Institut für Chemie, AG Elektrochemie, Technische Universität Chemnitz, Strasse der Nationen 62, D-09111 Chemnitz, Germany

ARTICLE INFO

Article history:
Received 7 April 2009
Received in revised form 20 May 2009
Accepted 21 June 2009
Available online 30 June 2009

Keywords:
Supercapacitor
$NaMnO_2$
Na^+
Electrochemical behavior
Aqueous electrolyte

ABSTRACT

A new cheap asymmetric supercapacitor based on activated carbon (AC) and $NaMnO_2$ as electrodes and aqueous Na_2SO_4 solution as electrolyte was assembled. It shows an energy density of 19.5 Wh kg^{-1} at a power density of 130 W kg^{-1} based on the total mass of the active electrode materials and an excellent cycling behavior. This asymmetric aqueous AC//$NaMnO_2$ capacitor is promising for practical applications due to its low price, easy preparation of $NaMnO_2$ and friendliness to environment.

1. Introduction

Electrochemical energy conversion and storage systems have been playing an important role in the progress of mankind including accommodation, transportation, military and space exploration [1]. Common and well-known batteries such as Zn//MnO_2, Zn//AgO, Ni-MH and lithium ion batteries are widely used for portable electronic devices such as communication, laptop computers, and consumer electronics. However, the progress of technology generates more and more tasks such as power leveling and electricity storage for renewable power sources [1,2]. In addition, environmental problems associated with the exhaust of vehicles becomes more and more serious. The use of zero-emission electric vehicles is becoming urgent to continue a sustainable development of our society. As a result, new and cheap chemical power sources as well as the exploration of new energy storage and conversion systems are of great importance.

Supercapacitors can be promising candidates as power sources of electric vehicles since their power density is very high (2–5 kW kg^{-1}). However, their energy density is very low (3–6 Wh kg^{-1}) [3]. Recently, hybrid systems were explored by utilizing the high energy density of batteries, especially lithium ion batteries, and high power density of supercapacitors [4–9]. In terms of safety, supercapacitors based on aqueous electrolytes are an excellent choice. In the case of hybrid supercapacitors using lithium intercalation compounds such as $LiMn_2O_4$ as cathode and activated carbon (AC) as anode, the solvation and desolvation of Li^+ becomes difficult at large current densities because the diameter of the solvated Li^+ is large. As a result, the energy density decreases very fast with rising current density. The high energy density of the intercalation compounds could not be utilized during rapid charge and discharge, which remains a challenging problem [10].

Asymmetric supercapacitors based on AC//MnO_2 are investigated most widely because of their good rate behavior, but most of them use amorphous MnO_2 as electrode material and the cycling performances is not good in the presence of dissolved oxygen [11–13]. Here we report on an asymmetric aqueous supercapacitor: AC//$NaMnO_2$. Crystalline $NaMnO_2$ was prepared by a solid state method and used as cathode material. First results show that this system has a high energy density even at high current densities, i.e. >10 Wh kg^{-1} at the rate of 1300 W kg^{-1}, and is promising for practical applications because of its low price and excellent cycling behavior in the aqueous electrolyte without removing the dissolved oxygen.

2. Experimental

$NaMnO_2$ was synthesized by ballmilling mixtures of Na_2CO_3 and MnO_2 (at a molar ratio of 1:2) for 12 h followed by heating at 870 °C for 10 h. The obtained particles were characterized using a Bruker Advance 8 powder X-ray diffractometer (XRD) with monochromatized Cu Kα radiation (λ = 1.54056 Å). SEM pictures were obtained with a Philip XL30 microscope operated at 25 kV. The positive elec-

* Corresponding author.
** Corresponding author. Tel.: +49 37153131509; fax: +49 37153121269.
E-mail addresses: wuyp@fudan.edu.cn (Y.P. Wu), rudolf.holze@chemie.tu-chemnitz.de (R. Holze).

0378-7753/$ – see front matter © 2009 Elsevier B.V. All rights reserved.
doi:10.1016/j.jpowsour.2009.06.068

trode was prepared by pressing a powdered mixture of $NaMnO_2$, acetylene black and poly(tetrafluoroethylene) (PTFE) in a weight ratio of 85:10:5 onto nickel grid. Activated carbon from Ningde Xinseng Chemical Industrial Ltd., Co. with a specific BET-surface area of about 2800 $m^2\,g^{-1}$ was used as received. The AC electrode was prepared in the same way as the positive electrode.

Cyclic voltammetry and galvanostatic charge–discharge tests of individual electrodes were performed using a three-electrode cell, in which Ni-grid and saturated calomel electrode (SCE) were used as counter and reference electrode, respectively. The asymmetric AC//$NaMnO_2$ capacitor test was performed in a two-electrode glass cell. An aqueous electrolyte solution of 0.5 mol l^{-1} Na_2SO_4 was used.

3. Results and discussion

XRD patterns of the original material MnO_2 and the as-prepared $NaMnO_2$ are shown in Fig. 1(a). The original material MnO_2 can be indexed as akhtenskite (ε-MnO_2, JCPDF No. 89-5171). After heating the mixtures of MnO_2 and Na_2CO_3 at high temperature, lamellar α-$NaMnO_2$ was obtained (JCPDF No. 25-0845). A diffractogramm peak located at 15.8° is ascribed to the impurity $Na_{0.7}MnO_2$ (JCPDF No. 27-0751), which also shows a lamellar structure. SEM images of $NaMnO_2$ are shown in Fig. 1(b) and (c). The as-prepared products are composed of many small plates and particles, and most of them aggregate together to form large spherical particles with an average diameter of about 50 μm. The BET specific surface area of $NaMnO_2$ is about 20 $m^2\,g^{-1}$.

Fig. 2 shows the cyclic voltammogramms (CV) of $NaMnO_2$ and AC electrode in 0.5 M Na_2SO_4 aqueous solution at a scan rate of 5 mV s^{-1}. The current collector (Ni-mesh) is very stable in the range $-1.0 < E_{SCE} < 1.2$ V in Na_2SO_4 aqueous solution. Hydrogen and oxygen evolution occur at $E_{SCE} < -1.0$ V and > 1.2 V, respectively, because of significant overpotentials consistent with results previously reported for aqueous Li_2SO_4 solution [14]. The CV of an AC electrode shows an ideal rectangular shape without any noticeable redox peaks from 0.1 to −0.8 V, which is characteristic of charging/discharging of the electric double layer capacitance [15,16]. In the potential range of 0–1.1 V the behavior of the $NaMnO_2$ electrode slightly deviates from the ideal rectangular shape with two small redox couples, indicative of the pseudocapacitance properties of $NaMnO_2$ cathode. These redox peaks are similar to that of $Na_xMnO_2{\cdot}H_2O$, which can be definitely ascribed to the intercalation-deintercalation of Na^+ into and from the solid lattice [17–19]. XRD patterns of $NaMnO_2$ electrode after the initial several electrochemical cycles (Fig. 3) show that $NaMnO_2$ indeed transformed to a layered birnessite-type structure $Na_xMnO_2{\cdot}H_2O$ with the typical diffraction peaks of (0 0 1) and (0 0 2), which usually shows a relatively higher capacitance than other types of crystalline MnO_2 materials [20,21]. Moreover, the CV curve of $NaMnO_2$ electrode is also symmetric with respect to the zero-current axis, which means that the faradic reactions of $NaMnO_2$ are reversible. As a result, an asymmetrical supercapacitor, AC//$NaMnO_2$, can be assembled by using Na_2SO_4 solution as electrolyte.

Fig. 4(a) shows the potential–time curves of the individual electrodes *vs.* the SCE reference electrode and the voltage–time profile of the asymmetric AC//$NaMnO_2$ (weight ratio of AC to $NaMnO_2$ is 1.2:1) supercapacitor at a current rate of 2 C. The AC anode presents a typical linear relationship with time, characteristic of electric double layer capacitance. The $NaMnO_2$ cathode shows slight deviation from the ideal line with some very short plateaus indicative of faradic processes. This is in agreement with results from CV (see above). The specific capacitance of AC and $NaMnO_2$ electrode is 119 and 140 F g^{-1}, respectively. The asymmetric supercapacitor shows a sloping voltage profile from 0 to 1.9 V with excellent reversibility. Although the specific capacitance of a single $NaMnO_2$ electrode is not as high as that of $Ni(OH)_2$, the specific capacitance (38.9 F g^{-1})

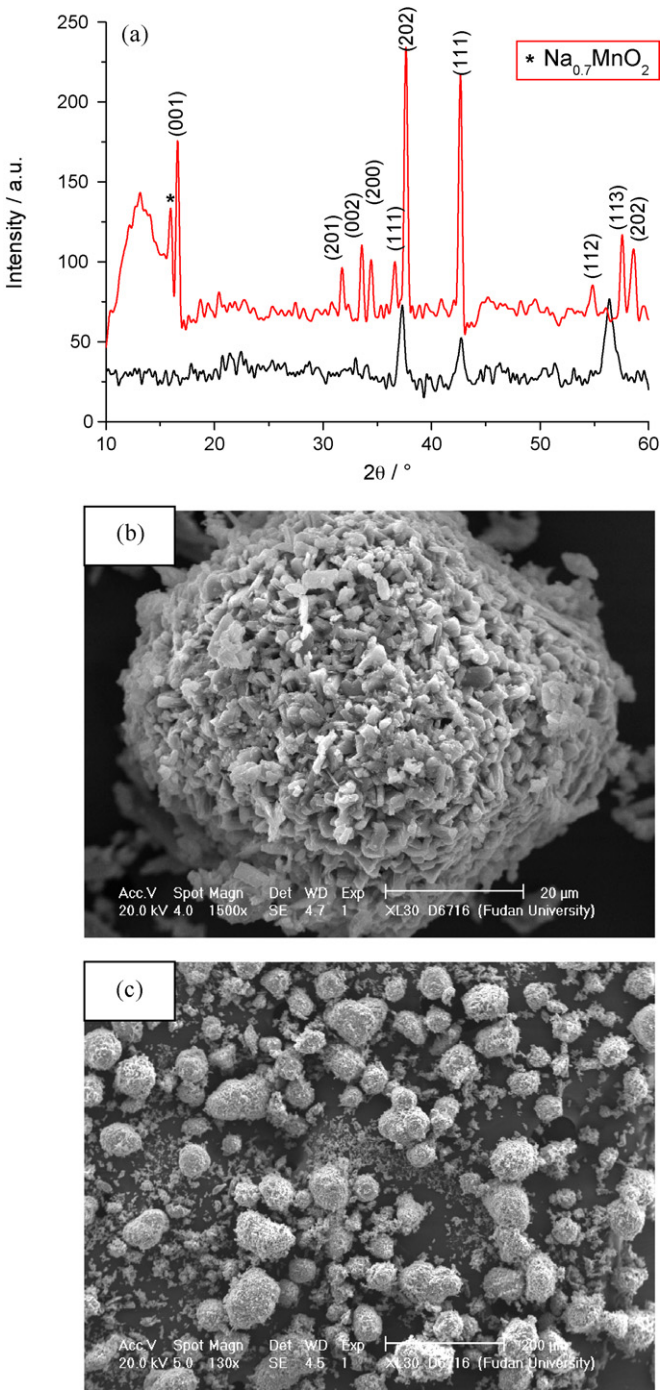

Fig. 1. (a) XRD and (b and c) SEM images of the as-prepared $NaMnO_2$.

and energy density (19.5 Wh kg^{-1}) of the AC//$NaMnO_2$ supercapacitor based on the total mass of the active electrode materials (including anode and cathode) is comparable to that of a supercapacitor AC/6 mol l^{-1} KOH/$Ni(OH)_2$. This may be due to the fact that an AC//$NaMnO_2$ supercapacitor has a usable capacitance in the entire operating voltage range (0–1.9 V), unlike AC/6 mol l^{-1} KOH/$Ni(OH)_2$, which only has usable capacitance in the voltage range 0.6–1.3 V [22].

The asymmetric AC//$NaMnO_2$ supercapacitor shows excellent cycling behavior (Fig. 4 (b)), only a slight capacitance loss (<3%) after 10,000 cycles at a current rate of 10 C between 0 and 1.9 V is observed. The coulombic efficiency of the capacitor remains at

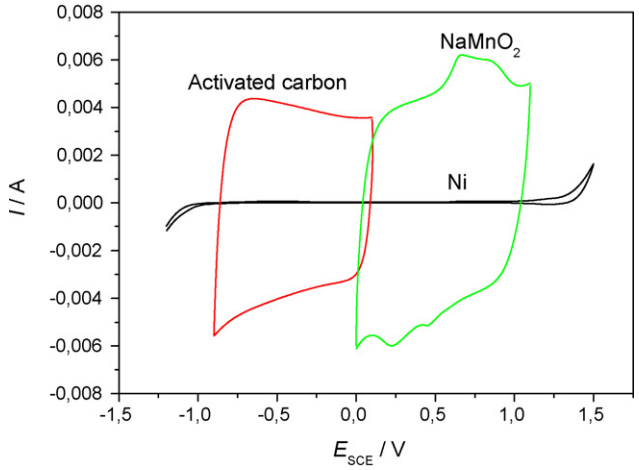

Fig. 2. Cyclic voltamogramms of activated carbon electrode and $NaMnO_2$ electrode in 0.5 mol l^{-1} Na_2SO_4 aqueous solution at a scan rate of 5 mV s^{-1}.

100% except for the initial cycles, suggesting that no gas evolution occurred in this voltage range. Obviously the AC anode stores energy in a nonfaradic manner with excellent cycle life. Although $NaMnO_2$ is transformed into birnessite-type structure during the initial cycles, the structure of layered $Na_xMnO_2{\cdot}H_2O$ is very stable during the long-term intercalation/deintercalation of Na^+ ions [17,23], which can be seen from the XRD patterns of $NaMnO_2$ electrode after 10,000 cycles (Fig. 3). In addition, as mentioned above, the crystallinity of $NaMnO_2$ is not high, which may also contribute to its excellent cycling performance.

The rate performances of the asymmetric supercapacitor were examined at various current rates ranging from 2 to 120 C (Fig. 4(c)). It shows a much higher energy density than the symmetric capacitor and at the same time it keeps a very good power density. For example, the energy density of the asymmetric supercapacitor is 19.5 Wh kg^{-1} at a power density of 130 W kg^{-1} and 13.2 Wh kg^{-1} at 1 kW kg^{-1}. This good behavior is due to the small radius of the hydrated Na^+ (0.358 nm), which is smaller than that of the hydrated Li^+ (0.382 nm), and also due to the higher ionic conductivity of Na^+ (50.1 cm^2 Ω^{-1} mol^{-1}) as compared to Li^+ (38.6 cm^2 Ω^{-1} mol^{-1}) [19,24–26]. If the particle sizes of $NaMnO_2$ and the activated carbon are optimized, even better performance will be achieved. Nevertheless the present behavior is already above the requirements for supercapacitors as power sources for EVs (15 Wh kg^{-1}). After 100,000 cycles, the estimated remaining capacitance will be above 80%. In addition, its cost is much lower than that of the present

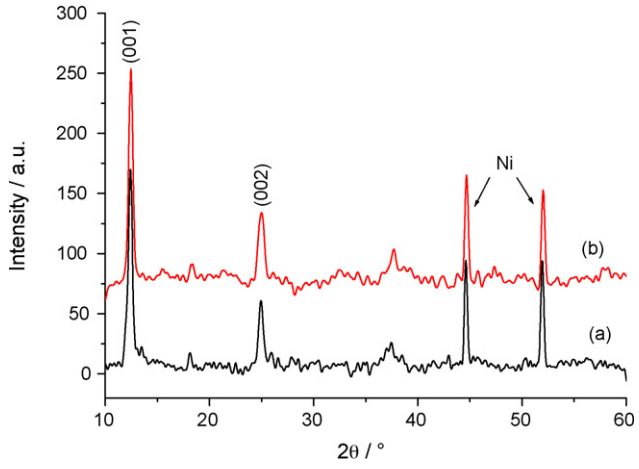

Fig. 3. XRD patterns of $NaMnO_2$ electrode after (a) 10 cycles and (b) 10,000 cycles.

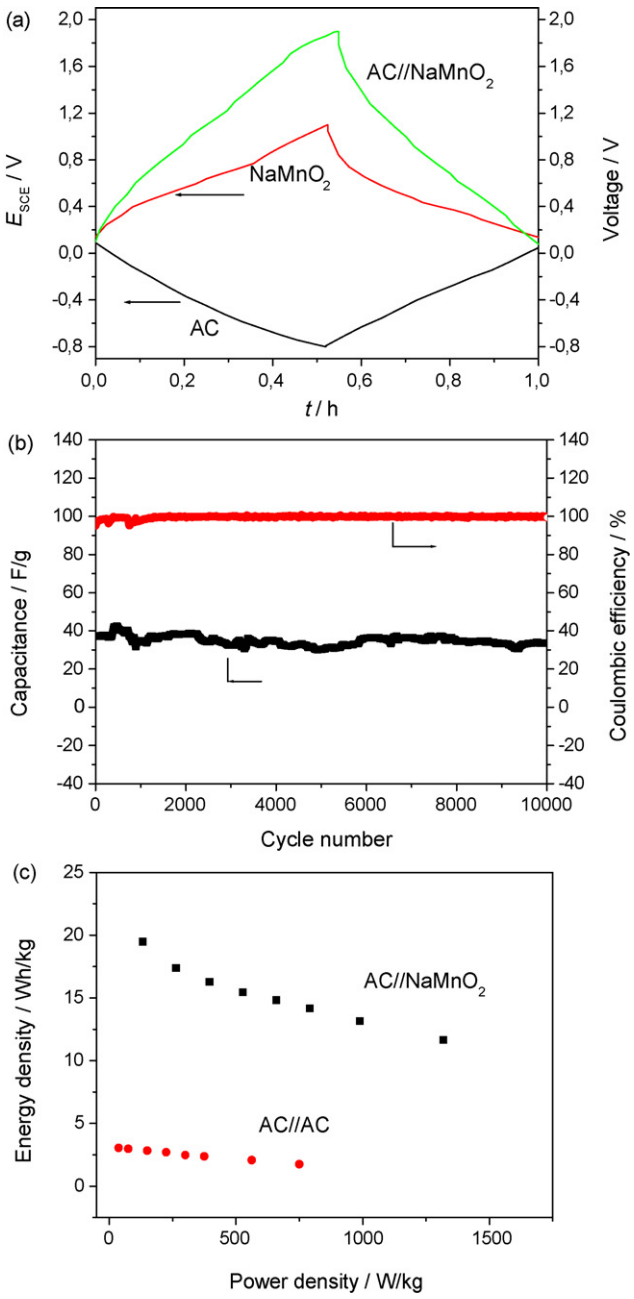

Fig. 4. (a) Potential–time curves of the individual electrode *vs.* SCE reference electrode and the voltage–time profile of the asymmetric AC//$NaMnO_2$ supercapacitor at a current rate of 2 C, (b) the cycling behavior and (c) Ragone plots of the asymmetric AC//$NaMnO_2$ supercapacitor.

supercapacitors, even that of AC//$LiMn_2O_4$, and the preparation of $NaMnO_2$ is easier than that of $LiMn_2O_4$ [4].

4. Conclusion

We describe an asymmetric supercapacitor with $NaMnO_2$ and activated carbon (AC) as cathode and anode, respectively, and an aqueous Na_2SO_4 solution as electrolyte. The asymmetric supercapacitor exhibits a sloping voltage–time curve in the entire voltage region of 0 to 1.9 V and delivers an energy density of 19.5 Wh kg^{-1} at a power density of 130 W kg^{-1} based on the total mass of the active electrode materials. It also shows excellent cycling behavior with not more than 3% capacitance loss after 10,000 cycles at a current rate of 10 C. This asymmetric aqueous AC//$NaMnO_2$ capacitor

has high application potential in electric vehicles and other large power devices since the electrolyte is environmentally benign, the cathode $NaMnO_2$ is easily available and the price is cheaper than that of $LiMn_2O_4$ and $Ni(OH)_2$.

Acknowledgments

Financial support from National Basic Research Program of China (973 Program No: 2007CB209702) and Alexander von Humboldt Foundation (Institutional Academic Cooperation Program) is greatly appreciated.

References

[1] Y.P. Wu, X.B. Dai, J.Q. Ma, Y.J. Cheng, Lithium Ion Batteries—Practice & Applications, Chemical Industry Press, Beijing, 2004.
[2] S. van der Linden, Energy 31 (2006) 3446.
[3] A.D. Pasquier, I. Plitz, J. Gural, F. Badway, G.G. Amatucci, J. Power Sources 136 (2004) 160.
[4] Y.G. Wang, Y.Y. Xia, Electrochem. Commun. 7 (2005) 1138.
[5] T. Brousse, R. Marchand, P.L. Taberna, P. Simon, J. Power Sources 158 (2006) 571.
[6] V. Ganesh, S. Pitchumani, V. Lakshminarayanan, J. Power Sources 158 (2006) 1523.
[7] H. Inoue, T. Morimoto, S. Nohara, Electrochem. Solid-State Lett. 10 (2007) A261.
[8] V. Khomenko, E. Raymundo-Piñero, F. Béguin, J. Power Sources 177 (2008) 643.
[9] G.G. Amatucci, F. Badway, A.D. Pasquier, T. Zheng, J. Electrochem. Soc. 148 (2001) A930.
[10] Q.T. Qu, P. Zhang, B. Wang, S. Tian, Y.P. Wu, R. Holze, J. Phys. Chem. B, in press.
[11] T. Brousse, P.L. Taberna, O. Crosnier, R. Dugas, P. Guillemet, Y. Scudeller, Y. Zhou, F. Favier, D. Bélanger, P. Simon, J. Power Sources 173 (2007) 633.
[12] T. Brousse, M. Toupin, D. Bélanger, J. Electrochem. Soc. 151 (2004) A614.
[13] M.S. Hong, S.H. Lee, S.W. Kim, Electrochem. Solid-State Lett. 5 (2002) A227.
[14] G.J. Wang, L.J. Fu, N.H. Zhao, L.C. Yang, Y.P. Wu, H.Q. Wu, Angew. Chem. Int. Ed. 46 (2007) 295;
G.J. Wang, L.J. Fu, N.H. Zhao, L.C. Yang, Y.P. Wu, H.Q. Wu, Angew. Chem. 117 (2007) 299.
[15] Q.T. Qu, B. Wang, L.C. Yang, Y. Shi, S. Tian, Y.P. Wu, Electrochem. Commun. 10 (2008) 1652.
[16] Z.B. Wen, Q.T. Qu, Q. Gao, Z.H. Hu, Y.P. Wu, X.W. Zheng, Y.F. Liu, X.J. Wang, Electrochem. Commun. 11 (2009) 715.
[17] L. Athouël, F. Moser, R. Dugas, O. Crosnier, D. Bélanger, T. Brousse, J. Phys. Chem. C 112 (2008) 7270.
[18] A. Mendiboure, C. Delmas, P. Hagenmuller, J. Solid State Chem. 57 (1985) 323.
[19] A. Caballero, L. Hernan, J. Morales, L. Sanchez, J. Santos, J. Solid State Chem. 174 (2003) 365.
[20] T. Brousse, M. Toupin, R. Dugas, L. Athouël, O. Crosnier, D. Bélanger, J. Electrochem. Soc. 153 (2006) A2171.
[21] S. Devaraj, N. Munichandraiah, J. Phys. Chem. C 112 (2008) 4406.
[22] J.H. Park, O.O. Park, K.H. Shin, C.S. Jin, J.H. Kim, Electrochem. Solid-State Lett. 5 (2002) H7.
[23] A.R. Armstrong, P.G. Bruce, Nature 381 (1996) 499.
[24] R.A. Huggins, Solid State Ionics 113–115 (1998) 533.
[25] R.N. Reddy, R.G. Reddy, J. Power Sources 124 (2003) 330.
[26] Y.U. Jeong, A. Manthiram, J. Electrochem. Soc. 149 (2002) A1419.